JACS
JOURNAL OF THE AMERICAN CHEMICAL SOCIETY
Communication
pubs.acs.org/JACS

Kr/Xe Separation over a Chabazite Zeolite Membrane

Xuhui Feng,[†] Zhaowang Zong,[†] Sameh K. Elsaidi,[‡] Jacek B. Jasinski,[§] Rajamani Krishna,[∥] Praveen K. Thallapally,*[,‡] and Moises A. Carreon*[,†]

[†]Chemical and Biological Engineering Department, Colorado School of Mines, Golden, Colorado 80401, United States
[‡]Pacific Northwest National Laboratory, Richland, Washington 99352, United States
[§]Conn Center for Renewable Energy Research, University of Louisville, Louisville, Kentucky 40292, United States
[∥]Van 't Hoff Institute for Molecular Sciences, University of Amsterdam, Science Park 904, 1098 XH Amsterdam, The Netherlands

Supporting Information

ABSTRACT: Herein we demonstrate that chabazite zeolite SAPO-34 membranes effectively separated Kr/Xe gas mixtures at industrially relevant compositions. Control over membrane thickness and average crystal size led to industrial range permeances and high separation selectivities. Specifically, SAPO-34 membranes can separate Kr/Xe mixtures with Kr permeances as high as 1.2×10^{-7} mol/m^2 s Pa and separation selectivities of 35 for molar compositions close to typical concentrations of these two gases in air. In addition, SAPO-34 membranes separated Kr/Xe mixtures with Kr permeances as high as 1.2×10^{-7} mol/m^2 s Pa and separation selectivities up to 45 for molar compositions as might be encountered in nuclear reprocessing technologies. Molecular sieving and differences in diffusivities were identified as the dominant separation mechanisms.

The separation of krypton from xenon is an industrially relevant problem. Kr and Xe are widely used in fluorescent light bulbs. High-purity Xe has been used in commercial lighting, medical imaging, anesthesia, and neuroprotection.[1] The current conventional technology produces these gases from the cryogenic distillation of air in which these noble gases are present in very small concentrations (1.14 ppmv Kr, 0.086 ppmv Xe).[2] Typically, both Kr and Xe separate into the oxygen-rich stream after distillation and are concentrated and purified to produce an 80/20 molar mixture of Kr to Xe.[3] This final mixture undergoes cryogenic distillation to produce pure Kr and pure Xe. However, cryogenic distillation is an energy-intensive and expensive process. In addition, separating Kr from Xe is an important issue for nuclear industries. Specifically, separating Kr from Xe is a critical step in removing radioactive ^{85}Kr during treatment of spent nuclear fuel.[3] Effectively separating Kr from Xe in nuclear reprocessing plants would lead to a considerable reduction in storage costs and in potential revenue generated from the sale of pure Xe. The conventional method to separate these two gases is fractional distillation at cryogenic temperatures, which is again an energy intensive process. Furthermore, even after cryogenic distillation, trace levels of radioactive Kr are too high to permit further use. Membrane technology could play a key role in making this separation less energy intensive and economically feasible. Membrane separation process is a viable energy-saving method since it does not involve any phase transformation; furthermore, the required membrane process equipment is simple and easy to operate, control, and scale-up.

Based on the kinetic diameter of Kr (3.69 Å) and Xe (4.10 Å), in principle, SAPO-34, a chabazite small pore zeolite silicoaluminophosphate displaying average pore size of 3.8 Å and having the composition $Si_xAl_yP_zO_2$ where $x = 0.01-0.98$, $y = 0.01-0.60$, and $z = 0.01-0.52$[4] represents an ideal candidate in membrane form to molecular sieve Kr from Xe. The first example of a continuous SAPO-34 membrane was reported almost two decades ago.[5] Since 1998, Noble and Falconer groups have pioneered and demonstrated the successful synthesis of high-performance SAPO-34 membranes able to efficiently separate diverse gas mixtures involving mainly CO_2, H_2, CH_4, and other light hydrocarbons.[6−15] The sharp molecular sieving properties of SAPO-34 membranes have been demonstrated for diverse industrial relevant molecular gas separations, including mainly CO_2/CH_4,[6−16] CO_2/N_2,[16,17] CO_2/butane,[15] and N_2/CH_4.[15,18−20] In all these cases, the smaller molecules diffuse rapidly through the pores of SAPO-34, while the larger molecules at most diffuse slowly, translating into high separation selectivities. Herein, we demonstrate the ability of SAPO-34 membranes to effectively separate Kr/Xe gas mixtures at industrially relevant compositions. SAPO-34 membranes were synthesized by secondary seeded growth on porous tubular α-Al_2O_3 supports at different molar ratios of water to allow membrane thickness control. Membrane synthesis procedure is given in the Supporting Information. The XRD patterns (Figure S1) of the SAPO-34 crystals collected from membrane synthesis were essentially identical for all water mole contents, and the peak position and intensity match those of the simulated chabazite topology typical of SAPO-34.[21] Figure 1 shows representative SEM images of SAPO-34 membranes synthesized with different water contents. Top view SEM images (Figure 1a−e) show well-intergrown and interconnected micron range zeolite crystals. Cross-sectional SEM images of the membranes (Figure 1a′−e′) show dense membrane layers with thickness ranging from ∼3.0 to ∼8.7 μm. The thickness of the membranes decreased as the water content increased.

SAPO-34 membranes were used to separate premixed 9:1 Kr/Xe (Kr rich composition). This composition is close to typical concentrations of these two gases in air and 9:91 Kr/Xe mixtures

Received: June 23, 2016
Published: July 27, 2016

DOI: 10.1021/jacs.6b06515
J. Am. Chem. Soc. 2016, 138, 9791−9794

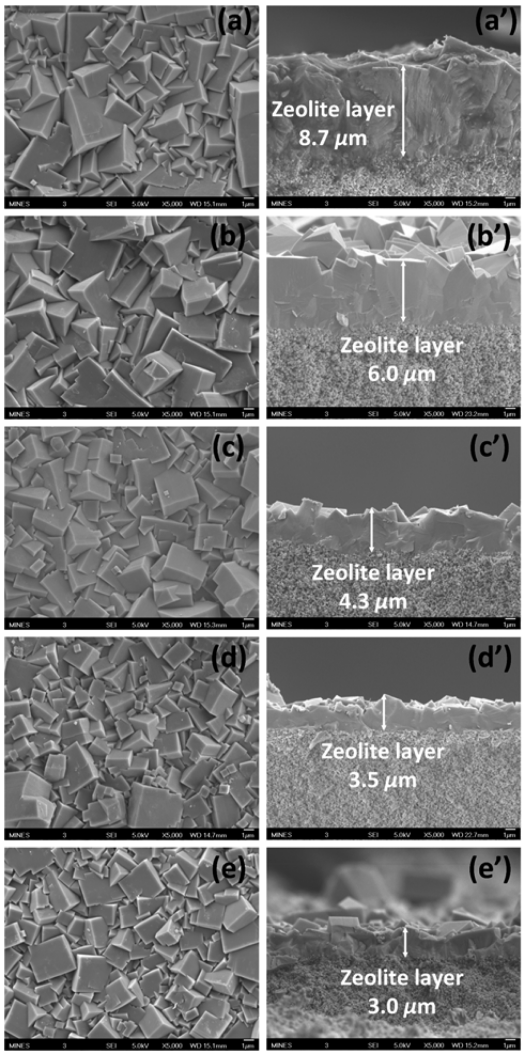

Figure 1. Top view (left) and cross-sectional SEM (right) images of SAPO-34 membranes. Gel composition: 1.0 Al_2O_3/1.0 P_2O_5/0.3 SiO_2/1.0 tetraethylammonium hydroxide (TEAOH)/1.6 dipropylamine (DPA)/x H_2O: (a,a′) x = 150, (b,b′) x = 200, (c,c′) x = 250, (d,d′) x = 300, and (e,e′) x = 350.

(Xe rich composition). This composition corresponds to that encountered in nuclear reprocessing technologies). The feed pressure was 223 kPa, and the pressure in the permeate side was 85 kPa. The separation results at room temperature for these membranes are shown in Table 1. For the Kr rich composition,

Table 1. Kr/Xe Separation Performance over SAPO-34 Membrane[a]

		feed molar composition: 9:1 Kr/Xe		feed molar composition: 9:91 Kr/Xe	
water content	membrane thickness (μm)	Kr permeance (mol/m^2 s Pa) × 10^{-7}	selectivity	Kr permeance (mol/m^2 s Pa) × 10^{-7}	selectivity
x = 150	8.7	0.19	13	0.19	14
x = 200	6.0	0.75	20	0.45	15
x = 250	4.3	1.0	35	0.87	45
x = 300	3.5	1.1	26	1.4	28
x = 350	3.0	1.2	31	1.8	44

[a]Transmembrane pressure = 138 kPa.

Kr permeances correlated well with membrane thicknesses (Figure S2). The thinner the membrane, the higher the Kr permeance. Kr permeances ranged from 0.19 to 1.2 × 10^{-7} mol/m^2 s Pa. Kr/Xe separation selectivities ranged from 13 to 35. In general, separation selectivities improved for the more diluted gel compositions. The best separation selectivities were observed for membranes with water molar contents of 250 and 350 (Figure S2). For the Xe rich composition, Kr permeances correlated well with membrane thicknesses too. Kr permeances increased as the thickness of the membrane decreased. Kr permeances ranged from 0.19 to 1.8 × 10^{-7} mol/m^2 s Pa. As compared to the Kr rich composition, for the Xe rich composition, Kr/Xe separation selectivities were slightly higher, ranging from 14 to 45. The highest separation selectivities were observed for membranes with water molar contents of 250 and 350 (Figure S2). A distinctive feature of the most Kr selective membranes for both gas mixture compositions, (water compositions 250, 300, and 350) is its smaller and narrower crystal size distribution as compared to the less selective membranes (water compositions 150 and 200). In principle, smaller crystal sizes close-pack better[11] leading to higher separation selectivities. The volcano-type behavior observed for the Kr/Xe separation selectivity (Figure S2) may indicate a coupled effect of crystal size and membrane on the Kr/Xe separation performance.

As shown in Figure S3, the two key parameters having a profound effect on Kr permeance and separation selectivities were membrane thickness and membrane average crystal size, respectively. Higher water content (x = 400) resulted in defective membranes that could not hold pressure for a transmembrane drop permeation measurement. In this case, intercrystalline boundaries around SAPO-34 crystals might have resulted in high concentration of defects. The observed high Kr permeances and moderate to high separation selectivities make these SAPO-34 membranes appealing for separating Kr from Xe at industrial relevant compositions. For any potential industrial applications, membrane reproducibility is a key prerequisite. As a representative example, Table S1 shows the separation performance for a premixed 9:1 Kr/Xe mixture of three membranes (x = 300) prepared independently. These membranes displayed similar separation indexes π in the 0.23−0.27 mol/m^2 s range, indicating good reproducibility. Separation index π [π = Kr permeance × (selectivity − 1) × permeate pressure] has been used as a reliable quantitative parameter to predict zeolite membrane reproducibility.[10]

Adsorption isotherms, isosteric heats of adsorption, and column breakthrough experiments were measured for Kr and Xe to help explain the separation mechanisms for the Kr selective membranes. Figure 2a shows the Kr and Xe adsorption isotherms collected at 298 and 278 K for SAPO-34 crystals. The adsorption isotherms at 140 kPa (~transmembrane pressure drop employed for the gas mixture separation experiments) revealed Xe uptakes of 39.9 cm^3/g (1.78 mmol/g) and 46.3 cm^3/g (2.07 mmol/g) at 298 and 278 K, respectively, and Kr uptakes of 14.7 cm^3/g (0.66 mmol/g) and 22.6 cm^3/g (1.01 mmol/g), respectively. Therefore, at 140 kPa and 298 K (prevailing conditions during separation experiments), SAPO-34 adsorbs ~2.7 times more Xe than Kr. Figure 2b shows the isosteric heats of adsorption (Q_{st}) for Kr and Xe calculated by Virial method, using the experimental single adsorption isotherms (Figures S4 and S5). At 1.4 bar, SAPO-34 crystals exhibited Q_{st} values of −24.4 and −17.3 kJ/mol for Xe and Kr, respectively, confirming the preferential adsorption of Xe over Kr on SAPO-34. These Q_{st} values are higher than those reported for activated carbon[22] and HKUST-

DOI: 10.1021/jacs.6b06515
J. Am. Chem. Soc. 2016, 138, 9791−9794

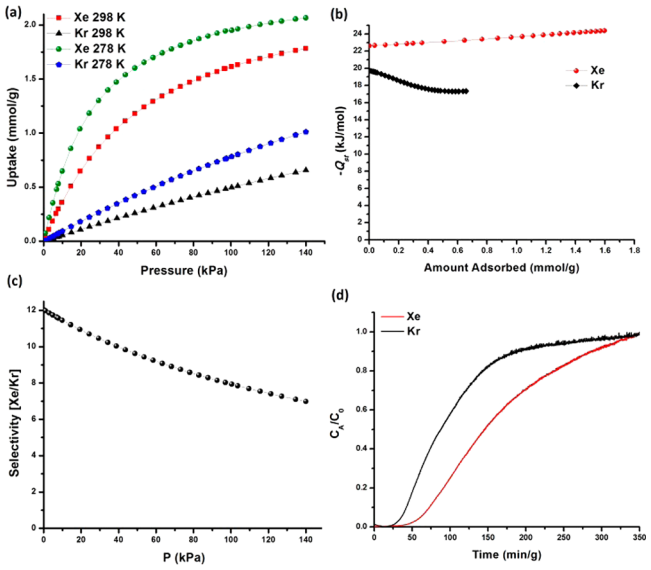

Figure 2. (a) Single component Xe and Kr adsorption isotherms collected at 298 and 278 ., (b) Xe and Kr isosteric heats of adsorption (Q_{st}) calculated by Virial method. (c) IAST calculated selectivity for 91:9 Xe/Kr gas mixture at 298 K. (d) Column breakthrough experiment for 91:9 Xe/Kr gas mixture at 298 K and 140 kPa for SAPO-34 crystals.

1[22−24] and comparable to those of Ni-MOF-74[22,23] and Mg-MOF-74.[23] Ideal adsorbed solution theory (IAST) was used to predict the selectivity of Xe over Kr binary mixture based on the experimental single adsorption isotherms collected at 298 K. The single-component isotherms were fit to a Langmuir−Freundlich eq (Figures S6 and S7). At 140 kPa and 298 K the adsorption selectivity for a 91:9 Xe/Kr binary gas mixture was calculated to be ∼7 (Figure 2c), confirming again that Xe adsorbs stronger than Kr. The preferential adsorption of Xe over Kr in SAPO-34 can be explained by differences in dipole polarizabilities of these two molecules. Xe has higher dipole polarizability (26.85−28.7 atomic units) as compared to Kr (16.44−18.0 atomic units).[25] Due to local electronegativity differences between framework Si, Al, and P, SAPO-34 has anionic framework with a net negative charge depending upon how the silicon substitution into the framework.[26] Therefore, stronger electrostatic interactions between the negatively charged SAPO-34 surface and the higher dipole moment of Xe promotes its preferential adsorption over Kr. The preferential adsorption of larger molecules over smaller molecules has been observed in chabazite zeolite crystals.[27] In addition, the preferential adsorption of Xe over Kr on different porous crystalline materials, including zeolites and metal−organic frameworks (MOFs), is well documented. For example, zeolite NaX has been used as a selective adsorbent for Xe over Kr with a selectivity of ∼6 with Kr concentrations ranging from 1 to 10,000 ppm.[3] Zeolite NaA displayed a selectivity of ∼4 for binary mixtures of Xe and Kr at 300 K between 100 and 1000 kPa.[28] Adsorption Xe selectivity over Kr has been observed in MOFs, too.[1,22,29−32] The leading sorbent material for Xe/Kr separation is the porous organic cage CC3, which was shown to separate 400 ppm Xe from 40 ppm Kr in air with a Xe/Kr selectivity of ∼20.4.[1] In the case of MOFs, the selectivity to Xe arised from the fact that Xe is a more polarizable molecule than Kr, which tends to form stronger van der Waals interactions with the open metal centers of MOFs. In the case of CC3, the selectivity to Xe was attributed to a precise size match between Xe and the organic cage cavity.

In principle, the preferential adsorption of Xe would favor separating Xe over Kr in the gas mixture. However, the smaller Kr molecule should diffuse faster than the larger Xe molecule. Column breakthrough experiments were conducted to learn about the relative diffusivity differences between Kr and Xe over SAPO-34 crystals (Figure 2d). For a 91:9 gas mixture at 298 K, the breakthrough time for Kr was 22 min, and for Xe, 39 min for 1 g of sample at flow rate of 1 mL/min and pressure of 140 kPa, indicating higher diffusivity of Kr over Xe. This was expected since Kr has lower capacity and affinity to SAPO-34 diffusing out from the column faster (breakthrough first), while Xe having higher affinity and capacity to SAPO-34 will breakthrough later. Therefore, differences in diffusivity favor the separation of Kr over Xe in the gas mixture. Differences in diffusivities leading to Kr/Xe ideal separation selectivities of ∼11.8 over SAPO-34 membranes grown on porous alumina disks have been reported.[33] Molecular gas mixtures can be separated over zeolite membranes by at least one of the following separation mechanisms: molecular sieving, differences in diffusivity, and competitive adsorption. Based on the kinetic diameter of Kr (3.69 Å) and Xe (4.10 Å), SAPO-34 membranes can separate these gases by molecular sieving. In addition, to this mechanism, breakthrough experiments (Figure 2d) demonstrate higher diffusivity of Kr over Xe. Since separation selectivities for gas mixtures (Table 1 and Table S2) are moderate, this suggests that Xe can permeate through the pores of SAPO-34. This is not surprising since hydrocarbons such as propane and *n*-butane, having kinetic diameters of ∼4.3 Å (slightly larger size than Xe molecule), can adsorb within the pores of SAPO-34.[34] Adsorption experiments show that Xe adsorbs more strongly than Kr on SAPO-34 crystals, favoring the separation of Xe over Kr in the gas mixture. Although competitive adsorption and diffusivity/molecular sieving compete as separation mechanisms, separation data suggest that diffusivity differences and molecular sieving are the two dominant mechanisms leading to highly permeable Kr selective membranes.

In order to gain further insights into intracrystalline diffusivities of Xe and Kr, we carried out simulations of membrane permeation and transient breakthroughs using the methodologies detailed in the literature.[35−37] The simulation details are included in the Supporting Information (Figure S8−S11). On the basis of the simulations, we can conclude that the membrane permeation experiments can be rationalized if the intracrystalline diffusivity of Kr is about 2 orders of magnitude higher than that of Xe. The transient breakthrough experiments also indicate that diffusivity of Kr is significantly higher than that of Xe.

Few membranes have been proposed to separate Kr and Xe (Table S2). However, all these membranes have been evaluated only for *single gas* permeation experiments and not for *gas mixtures*. Furthermore, these membranes show low *ideal* separation selectivities and low Kr permeances.

A membrane prepared with 350 mol water content was evaluated for the molar gas mixture composition of 9:91 Kr/Xe at transmembrane pressure of 700 kPa, which is the typical pressure at which Kr and Xe may enter to the column cryogenic distillation process.[38] As expected, and mainly due to concentration polarization, both Kr permeance and Kr/Xe separation selectivity decreased to 0.19×10^{-7} mol/m^2 s Pa and 13, respectively. Despite this decrease, SAPO-34 membranes still display moderate Kr permeances and Kr/Xe separation selectivities at such high pressure.

DOI: 10.1021/jacs.6b06515
J. Am. Chem. Soc. 2016, 138, 9791−9794

In summary, we have demonstrated the ability of SAPO-34 membranes to effectively separate Kr/Xe gas mixtures at industrially relevant compositions. Membrane thickness and average crystal size were key parameters that profoundly affected membrane separation performance. Thinner membranes with smaller and narrower crystal size led to industrial range permeances and high separation selectivities. SAPO-34 membranes separated Kr/Xe mixtures with Kr permeances as high as 1.2×10^{-7} mol/m^2 s Pa and separation selectivities of 35 for molar compositions close to typical concentrations of these two gases in air. In addition, SAPO-34 membranes separated Kr/Xe mixtures with Kr permeances as high as 1.2×10^{-7} mol/m^2 s Pa and separation selectivities up to 45 for molar compositions as might be encountered in nuclear reprocessing technologies. Diffusivity differences and molecular sieving were the two dominant separation mechanisms. The high Kr permeances and high separation selectivities make these membranes appealing for separating Kr/Xe mixtures at industrial relevant compositions, and potentially as a more economic and less energy intensive alternative to cryogenic distillation, the benchmark technology used to separate these gas mixtures.

■ ASSOCIATED CONTENT

Supporting Information

The Supporting Information is available free of charge on the ACS Publications website at DOI: 10.1021/jacs.6b06515.

Experimental methods and gas sorption studies/calculations (PDF)

■ AUTHOR INFORMATION

Corresponding Authors

*praveen.thallapally@pnnl.gov

*mcarreon@mines.edu

Notes

The authors declare no competing financial interest.

■ ACKNOWLEDGMENTS

We gratefully acknowledge the financial support by the Department of Energy (DOE) Nuclear Energy University Program (NEUP) under Grant No. DE-NE0008429.

■ REFERENCES

(1) Chen, L.; Reiss, P. S.; Chong, S. Y.; Holden, D.; Jelfs, K. E.; Hasell, T.; Little, M. A.; Kewley, A.; Briggs, M. E.; Stephenson, A.; Thomas, K. M.; Armstrong, J. A.; Bell, J.; Busto, J.; Noel, R.; Liu, J.; Strachan, D. M.; Thallapally, P. K.; Cooper, A. I. *Nat. Mater.* **2014**, *13*, 954−960.

(2) Kerry, F. G. *Industrial Gas Handbook: Gas Separation and Purification*; CRC Press/Taylor & Francis Group: Boca Raton, FL, 2007.

(3) Izumi, J. Waste gas treatment using zeolites in nuclear-related industries. In *Handbook of Zeolite Science and Technology*; Auerbach, S. M., Carrado, K. A., Dutta, P. K., Eds.; Marcel Dekker, New York, 2003.

(4) Szostak, R. *Molecular Sieves-Principles of Synthesis and Identification*; Van Nostrand Reinhold: New York, 1989.

(5) Lixiong, Z.; Mengdong, J.; Enze, M. *Stud. Surf. Sci. Catal.* **1997**, *105*, 2211−2216.

(6) Poshusta, J. C.; Tuan, V. A.; Falconer, J. L.; Noble, R. D. *Ind. Eng. Chem. Res.* **1988**, *37*, 3924−3929.

(7) Poshusta, J. C.; Tuan, V. A.; Pape, E. A.; Noble, R. D.; Falconer, J. L. *AIChE J.* **2000**, *46*, 779−789.

(8) Ping, E. W.; Zhou, R.; Funke, H. H.; Falconer, J. L.; Noble, R. D. *J. Membr. Sci.* **2012**, *415−416*, 770−775.

(9) Zhou, R.; Ping, E. W.; Funke, H. H.; Falconer, J. L.; Noble, R. D. *J. Membr. Sci.* **2013**, *444*, 384−393.

(10) Carreon, M. A.; Li, S.; Falconer, J. L.; Noble, R. D. *Adv. Mater.* **2008**, *20*, 729−732.

(11) Carreon, M. A.; Li, S.; Falconer, J. L.; Noble, R. D. *J. Am. Chem. Soc.* **2008**, *130*, 5412−5413.

(12) Li, S.; Falconer, J. L.; Noble, R. D. *Adv. Mater.* **2006**, *18*, 2601−2603.

(13) Li, S.; Falconer, J. L.; Noble, R. D. *J. Membr. Sci.* **2004**, *241*, 121−135.

(14) Funke, H. H.; Chen, M. Z.; Prakash, A. N.; Falconer, J. L.; Noble, R. D. *J. Membr. Sci.* **2014**, *456*, 185−191.

(15) Wu, T.; Diaz, M. C.; Zheng, Y.; Zhou, R.; Funke, H. H.; Falconer, J. L.; Noble, R. D. *J. Membr. Sci.* **2015**, *473*, 201−209.

(16) Venna, S. R.; Carreon, M. A. *Langmuir* **2011**, *27*, 2888−2894.

(17) Li, S.; Fan, C. Q. *Ind. Eng. Chem. Res.* **2010**, *49*, 4399−4404.

(18) Huang, Y.; Wang, L.; Song, Z.; Li, S.; Yu, M. *Angew. Chem.* **2015**, *127*, 10993−10997.

(19) Li, S.; Zong, Z.; Zhou, S. J.; Huang, Y.; Song, Z.; Feng, X.; Zhou, R.; Meyer, H. S.; Yu, M.; Carreon, M. A. *J. Membr. Sci.* **2015**, *487*, 141−151.

(20) Zong, Z.; Feng, X.; Huang, Y.; Song, Z.; Zhou, R.; Zhou, S. J.; Carreon, M. A.; Yu, M.; Li, S. *Microporous Mesoporous Mater.* **2016**, *224*, 36−42.

(21) Szostak, R. *Handbook of Molecular Sieves*; Van Nostrand Reinhold: New York, 1992; p 416.

(22) Liu, J.; Thallapally, P. K.; Strachan, D. *Langmuir* **2012**, *28*, 11584−11589.

(23) Perry, J. J., IV; Teich-McGoldrick, S. L.; Meek, S. T.; Greathouse, J. A.; Haranczyk, M.; Allendorf, M. D. *J. Phys. Chem. C* **2014**, *118*, 11685−11698.

(24) Soleimani Dorcheh, A.; Denysenko, D.; Volkmer, D.; Donner, W.; Hirscher, M. *Microporous Mesoporous Mater.* **2012**, *162*, 64−68.

(25) Maroulis, G.; Thakkar, A. J. *J. Chem. Phys.* **1988**, *89*, 7320−7323.

(26) Lok, B. M.; Messina, C. A.; Patton, R. L.; Gajek, R. T.; Cannan, T. R.; Flanigen, E. M. *J. Am. Chem. Soc.* **1984**, *106*, 6092−6093.

(27) Shang, J.; Li, G.; Singh, R.; Gu, Q.; Nairn, K. M.; Bastow, T. J.; Medhekar, N.; Doherty, C. M.; Hill, A. J.; Liu, J. Z.; Webley, P. A. *J. Am. Chem. Soc.* **2012**, *134*, 19246−19253.

(28) Jameson, C. J.; Jameson, A. K.; Lim, H.-M. *J. Chem. Phys.* **1997**, *107*, 4364−4372.

(29) Bae, Y.-S.; Hauser, B. G.; Colón, Y. J.; Hupp, J. T.; Farha, O. K.; Snurr, R. Q. *Microporous Mesoporous Mater.* **2013**, *169*, 176−179.

(30) Wang, H.; Yao, K.; Zhang, Z.; Jagiello, J.; Gong, Q.; Han, Y.; Li. *J. Chem. Sci.* **2014**, *5*, 620−624.

(31) Liu, J.; Strachan, D. M.; Thallapally, P. K. *Chem. Commun.* **2014**, *50*, 466−468.

(32) Ryan, P. J.; Farha, O. K.; Broadbelt, L. J.; Snurr, R. Q.; Bae, Y.-S. Metal−organic frameworks for Xe/Kr separation. U.S. Patent 13,947,406, 2014.

(33) Crawford, P. G. Zeolite membranes for the separation of krypton and xenon from spent nuclear fuel reprocessing off-gas. MS Thesis, Georgia Institute of Technology, Atlanta, GA, 2013.

(34) Agarwal, K.; John, M.; Pai, S.; Newalkar, B. L.; Bhargava, R.; Choudary, N. V. *Microporous Mesoporous Mater.* **2010**, *132*, 311−318.

(35) Krishna, R. *Microporous Mesoporous Mater.* **2014**, *185*, 30−50.

(36) Krishna, R. *Phys. Chem. Chem. Phys.* **2016**, *18*, 15482−15495.

(37) Krishna, R. *RSC Adv.* **2015**, *5*, 52269−52295.

(38) Cabe, J. E.; Bearden, M. D.; Brown, D. R.; Thallapally, P. K.; Strachan, D. M. A preliminary economic study on the use of Metal-Organic-Framework (MOF) materials for Kr capture. Pacific Northwest National Laboratory, US Department of Energy report FCRD-SWF-2014-000035, June 2014.

DOI: 10.1021/jacs.6b06515
J. Am. Chem. Soc. 2016, 138, 9791−9794